Available online at www.sciencedirect.com
SCIENCE DIRECT®
Bioelectrochemistry 60 (2003) 57–64
Bioelectrochemistry
www.elsevier.com/locate/bioelechem

Voltammetric and spectroelectrochemical characterization of a water-soluble viologen polymer and its application to electron-transfer mediator for enzyme-free regeneration of NADH

Hajime Karatani[a,*], Naohisa Wada[b], Tohru Sugimoto[c]

[a] *Department of Polymer Science and Engineering, Kyoto Institute of Technology, Sakyo, Kyoto 606-8585, Japan*
[b] *Faculty of Life Science, Toyo University, Itakura-machi, Gunma 374-0193, Japan*
[c] *Laboratory of Biophysics, School of Engineering, Kanto Gakuin University, Kanazawa, Yokohama 236-8501, Japan*

Received 8 November 2002; received in revised form 25 March 2003; accepted 1 April 2003

Abstract

A water-soluble polyxylylviologen (PXV^{2+}) was characterized with a view to making use of it as a redox electron-transfer (ET) mediator. Cyclic voltammetric and spectropotentiometric studies showed (i) that PXV^{2+} gives two redox waves centering at −0.40 and −0.83 V (vs. Ag/AgCl (3.3 mol dm^{-3} KCl)) and (ii) that the lifetime of its monocation radical ($PXV^{+\cdot}$) is two orders of magnitude greater than that of the well-utilized dimethyl viologen monocation radical. Subsequently, the reaction of the $PXV^{2+/+\cdot}$ couple with NAD^+ was evaluated in the similar manners as above. On the basis of this evaluation and the bioluminescence assay using bacterial NADH/FMN oxidoreductase and luciferase, it was shown (i) that the $PXV^{2+/+\cdot}$ couple functions as a useful electron-transfer mediator and (ii) that $PXV^{+\cdot}$ reacts with NAD^+, leading to generation of the enzymatically active NADH, in the absence of any reductases.

Keywords: Viologen; Electron transfer; Mediator; NAD^+; NADH; Bacterial bioluminescence

1. Introduction

The redox couple of viologen (V^{2+}) and its monocation radical ($V^{+\cdot}$), represented by the *N*,*N*′-dimethyl-4,4′-bipyridinium (dimethyl viologen, MV^{2+}) redox couple, has been extensively studied from a viewpoint of the electron-transfer (ET) mediator aiming at application to sensors [1–3], photosensitizing systems [4–7], characterization of microorganism [8] and syntheses of a variety of useful compounds [7,9–16].

Since $V^{+\cdot}$ can readily be electrogenerated from its parent dication, the $V^{2+/+\cdot}$ couple has been successfully utilized in combination with the electrode. However, in terms of the electron-transfer capability, there seems to be a drawback that the $V^{+\cdot}$ species are generally labile at the solution–electrode interface because of being amenable to the radical annihilation and/or the deposition onto the electrode [17–20]. Coating either the polymeric viologen or the viologen-containing polymer onto the electrode seems to be a profitable approach for overcoming the drawback [1,3,5,6,13]. The chemical modification of viologen derivatives onto the electrode based on the self-assembling technique would also be promising to utilize the $V^{2+/+\cdot}$ couple [21,22]. In relation to these approaches, encapsulation of the MV^{2+} mediator system within porous graphite electrode in the presence of an ion-exchange resin is noteworthy [14]. Thus, to make full use of the viologen mediator system, its immobilization or fixing onto the electrode has often been necessary.

The reducing power of $V^{+\cdot}$ is not always potent enough to transfer its electron to the acceptor of interest. For example, in the regeneration of nicotinamide adenine dinucleotide in reduced form (NADH) from its oxidized form (NAD^+), having attracted much attentions in terms of the cofactor regeneration [7,23], an adequate MV-dependent NAD reductase is usually required to complete the reduction of NAD^+ with the aid of the viologen mediator [11,15,16].

In this study, with focus on the stability and the reducing ability of the $V^{2+/+\cdot}$ couple, we characterized a water-soluble viologen polymer, polyxylylviologen (herein abbre-

* Corresponding author. Tel./fax: +81-75-724-7826.
E-mail address: karatani@ipc.kit.ac.jp (H. Karatani).

1567-5394/03/$ - see front matter © 2003 Elsevier Science B.V. All rights reserved.
doi:10.1016/S1567-5394(03)00048-3

viated to PXV^{2+}), with a view to using it as an electron-transfer mediator. This is not only because the PXV^{2+} polymer matrix is anticipated to be favorable for protecting its radical species from annihilation but also because the PXV^{2+} molecule seems to provide a suitable hydrophobic microenvironment to facilitate the ET reaction. First, we studied the redox properties of PXV^{2+}. Subsequently, on a trial basis, we evaluated a possibility that the PXV^{2+} mediator system can be available for the enzyme-free regeneration of NADH from NAD^+.

2. Experimental details

2.1. Materials

PXV^{2+} was synthesized as a bromide salt according to the literature method [24]. The equimolar mixture of 4,4′-bipyridyl and α,α′-dibromoxylene in acetonitrile (5 wt.%) was stirred for 18 h at room temperature. The resulting yellowish deposits were collected on a Nucleopore® filter (pore size, 0.2 μm) and then washed with acetonitrile, methanol and diethylether in this order. The molar mass was estimated at about 11,000 by a gel filtration chromatography on a Pack Diol-120 (500 × 8.0 mm i.d., YMC, Kyoto, Japan). PXV^{2+} was estimated to carry about 3.3-viologen unit per molecule on the basis of the potentiospectroscopic measurement. MV^{2+} chloride salt was obtained from Wako (Osaka, Japan) and was comparatively characterized as a typical viologen. KCl, used as a supporting electrolyte, was Merck's Suprapur® grade (Darmstadt, Germany). NAD^+ was purchased from Oriental Yeast (Osaka, Japan). Riboflavin 5′-phosphate (FMN) was received from Sigma-Aldrich (St. Louis, MO, USA). Poly(2-acrylamido-2-methyl-1-propanesufonic acid) (10 wt.% in water) (abbreviated to $PAASO_3^-$) was purchased from Kanto Chemicals (Tokyo, Japan). Both luciferase and NADH/FMN oxidoreductase were isolated from the cells of *Photobacterium phosphoreum* strain bmFP according to the protocol reported previously [25]. All other chemicals were of the highest commercial grade available. Water was deionized and distilled in glass.

2.2. Cyclic stationary-electrode voltammetry

The cyclic voltammetric measurement was carried out by using a Model HSV-100 automatic polarization system (Hokuto Denko, Tokyo, Japan). An Au electrode (1.0 mm i.d., BAS, Tokyo Japan) was used as the working electrode. The auxiliary electrode was a Pt wire and the potential was monitored with respect to an Ag/AgCl (3.3 mol dm^{-3} KCl) reference electrode, unless otherwise specified. The working electrode was pretreated with a potential scan between − 1.1 and 0.9 V at 50 mV s^{-1} for 5 min in 0.1 mol dm^{-3} KCl prior to each individual measurement. Each sample solution (8.0 ml) was bubbled with Ar for 10 min.

2.3. Spectropotentiometric measurement

To fabricate an optically transparent thin layer electrochemical (OTTLE) cell, a 100-mesh Au gauze was inserted between two quartz plates (9 × 30 mm; 1 mm in thickness). The OTTLE cell was placed at a right angle to the spectrophotometer's light beam in a sample cup (sample volume, 400 μl). An Ag wire insulated with a Teflon® tubing, further sheathed inside a Pt pipe, was used as the quasi-reference electrode and the exterior Pt pipe was used as the auxiliary electrode [26]. The potential of the Ag-quasi-reference electrode was determined to be ca. +0.34 V vs. Ag/AgCl (3.3 mol dm^{-3} KCl). The light-path length of the OTTLE cell was determined to be ca. 0.9 mm on the basis of the absorbance measurement of FMN. Absorption spectra were taken by a Model MultiSpec-1500 spectrophotometer equipped with a photodiode array detector (Shimadzu, Kyoto, Japan). The blank for the spectral measurement was the OTTLE cell filled with water.

Prior to the in situ spectral measurement, the potential was held at 0.0 V (vs. Ag-quasi-reference electrode) for 20 s. Subsequently, the potential was stepped up to a given potential and held at this value for 120 s. The absorption spectra were recorded at 5-s intervals during the potential application and in the period of 280 s after the potential application was stopped. The absorbance at given wavelengths at any time was extracted from the accumulated digital data of each individual time-resolved absorption spectrum and plotted against the time.

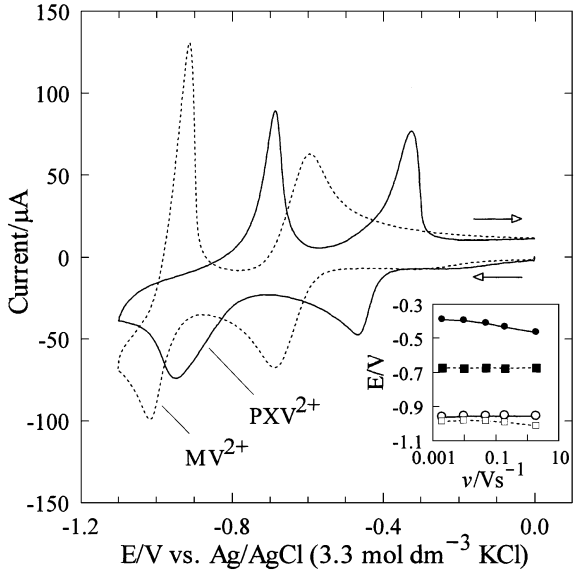

Fig. 1. Cyclic voltammograms of 0.1 mol dm^{-3} KCl solution containing either 2.0 mmol dm^{-3} MV^{2+} or 60 μmol dm^{-3} PXV^{2+}. Potential scan started negatively from 0.0 V at scan rate of 2 V s^{-1}. O_2 was eliminated by bubbling with Ar. Inset, the plot of the potential for the cathodic wave maxima vs. the potential scan rate (v) (in logarithmic scale). Closed circle, 1st peak for PXV^{2+}; open circle, 2nd peak for PXV^{2+}; closed square, 1st peak for MV^{2+}; open square, 2nd peak for MV^{2+}.

2.4. Bioluminescence assay

The assay, based on the following reactions [27], was conducted to see whether the enzymatically active NADH is formed in the reaction with the PXV^{2+} mediator system.

$$NADH + FMN + H^{+} \xrightarrow{\text{NADH/FMN oxidoreductase}} NAD^{+} + FMNH_2 \quad (1)$$

$$FMNH_2 + O_2 + RCHO \xrightarrow{\text{luciferase}} FMN + H_2O + RCOOH + hv\ (\sim 490\ nm) \quad (2)$$

where RCHO is a long-chain aliphatic aldehyde and RCOOH is the corresponding fatty acid. To carry out the assay, the mixture of NAD^{+} and PXV^{2+} in 0.1 mol dm^{-3} KCl was first electrolyzed at a fixed potential (-0.7, -0.9 and -1.1 V) at the Au electrode for 10 min with agitation. A sample solution volume was 8.0 ml and the initial concentrations of NAD^{+} and PXV^{2+} were 4.0 mmol dm^{-3} and 50 μmol dm^{-3}. After cessation of the potential application, a 500-μl aliquot of the resulting mixture was withdrawn using a microsyringe at the regular time intervals. To the mixture withdrawn, 25 μl of 1.0 wt.% $PAASO_3^-$, diluted with water from its 10 wt.% solution, was added to precipitate PXV^{2+} as the polyion complex with $PAASO_3^-$ and then the precipitates were removed by centrifugation at 4000 rpm for 5 min because PXV^{2+} made the bacterial luciferase inactive by complexation with luciferase. A 470-μl supernatant was then manually injected into a 500-μl mixture containing NADH/FMN oxidoreductase, luciferase, FMN and tetradecanal in the air-equilibrated 0.1 mol dm^{-3} Na/K phosphate buffer solution (pH 7.2). The concentrations of luciferase, FMN and tetradecanal in the mixture were 8, 28 and 160 μmol dm^{-3}, respectively. The activity of NADH/FMN oxidoreductase used was 5.5 μmol min^{-1}, determined by the literature method [28], and this activity was high enough to occur the peak light emission by injecting the pretreated mixture mentioned above. The light emission was recorded as a function of time by a homemade computer-controlled photon detecting system [26].

3. Results

3.1. Voltammetric properties

Fig. 1 shows the representative cyclic voltammograms of 0.1 mol dm^{-3} KCl solution containing either 2.0 mmol

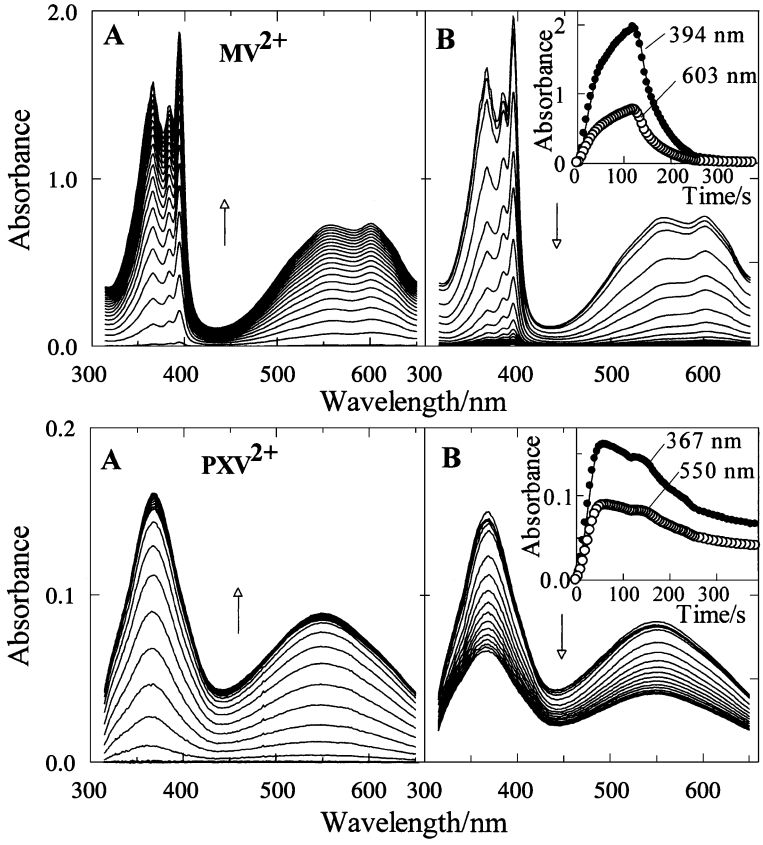

Fig. 2. In situ absorption spectra for 0.1 mol dm^{-3} KCl solutions containing 2.0 mmol dm^{-3} MV^{2+} (upper panel) and 60 μmol dm^{-3} PXV^{2+} (lower panel). Potential applied, -1.1 V vs. Ag-quasi-reference electrode (corresponding to ca. -0.76 V vs. Ag/AgCl (3.3 mol dm^{-3} KCl)). The potential was applied for the initial 2 min and then stopped. (A) During the potential application; (B) after cessation of the potential application. Inset, time courses for the absorbance at the given wavelengths.

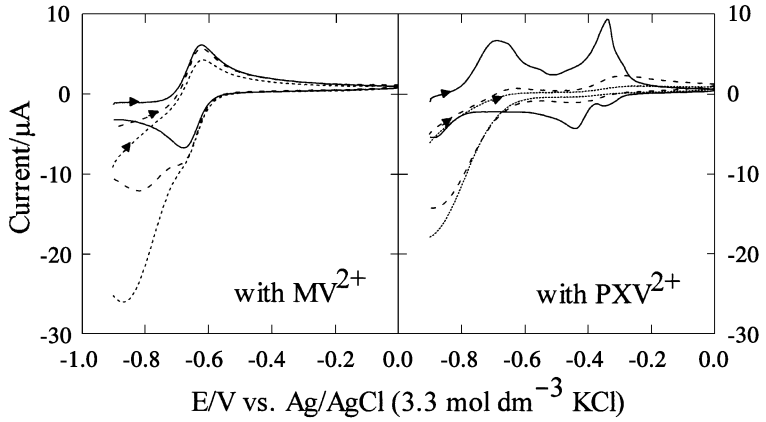

Fig. 3. Representative cyclic voltammograms of the mixture of NAD^+ with either MV^{2+} (2.0 mmol dm^{-3}) or PXV^{2+} (60 μmol dm^{-3}) in 0.1 mol dm^{-3} KCl, monitored with 50 mV s^{-1} of the scan rate. Prior to the positively potential scan, the potential was held at −0.9 V for 60 s. Solid curve, MV^{2+} or PXV^{2+} alone; dashed curve, with 2.0 mmol dm^{-3} NAD^+; dotted curve, with 8.0 mmol dm^{-3} NAD^+. O_2 was eliminated by bubbling with Ar.

dm^{-3} MV^{2+} as a representative viologen or 60 μmol dm^{-3} PXV^{2+} (viologen moiety concentration ≈ 0.2 mmol dm^{-3}). For PXV^{2+}, two redox waves centering at −0.40 and −0.83 V appeared during the potential scan in the range of 0.0 to −1.1 V, while two redox waves centering at −0.64 and −0.96 V were formed in the system with MV^{2+}. The potential difference between the two peak potentials (ΔE_p) were 133 and 262 mV for 1st and 2nd waves in the system with PXV^{2+}. The corresponding ΔE_p values for the MV^{2+} system were 78 and 107 mV. The peak potentials for first and second cathodic waves are plotted against the potential scan rate in Fig. 1 (inset).

3.2. Spectropotentiometric properties

As seen in the in situ absorption spectra (Fig. 2), the broad visible band with a maximum at 603 nm and the narrow bands peaking at 367, 384 and 394 nm arose during application of −1.1 V (vs. Ag-quasi-reference electrode) to the OTTLE cell filled with 0.1 mol dm^{-3} KCl solution containing 2.0 mmol dm^{-3} MV^{2+}. By stopping the potential application, all bands were decreased in a similar fashion and each time course could be analyzed on the basis of the quasi-first-order kinetics, exhibiting the apparent decay rate constants (k_{app}) of about 2.3×10^{-2} s^{-1}.

For the system with PXV^{2+}, two bands peaking at 367 and 550 nm occurred during application of −1.1 V (vs. Ag-quasi-reference electrode) and rose faster as compared with the case of the reduction of MV^{2+}. Noticeably, the time course for the absorbance decay in the system with PXV^{2+} significantly differed from that in the system with MV^{2+}. As indicated in Fig. 2 (inset), the decrease in absorbance apparently stopped for about 10 s before cutting off the potential application and then began to slowly decrease in a similar fashion with k_{app} of about 4.9×10^{-4} s^{-1}.

3.3. Electrode process for the NAD+-viologen mixture

Subsequently, the cyclic stationary-electrode voltammetry was carried out in the NAD^+ system with either MV^{2+} or PXV^{2+}. Fig. 3 shows the representative cyclic voltammogram of the mixture of NAD^+ with either MV^{2+} or PXV^{2+} in 0.1 mol dm^{-3} KCl. Prior to the potential scan, the electrode potential was maintained at −0.9 V for 60 s to produce $V^{+\cdot}$ for the subsequent mediated reaction with NAD^+ and/or $NAD^{\cdot}$. This pretreatment process was important to initiate the $V^{+\cdot}$ mediated reaction. An important observation was that the peak anodic currents at −0.33 V

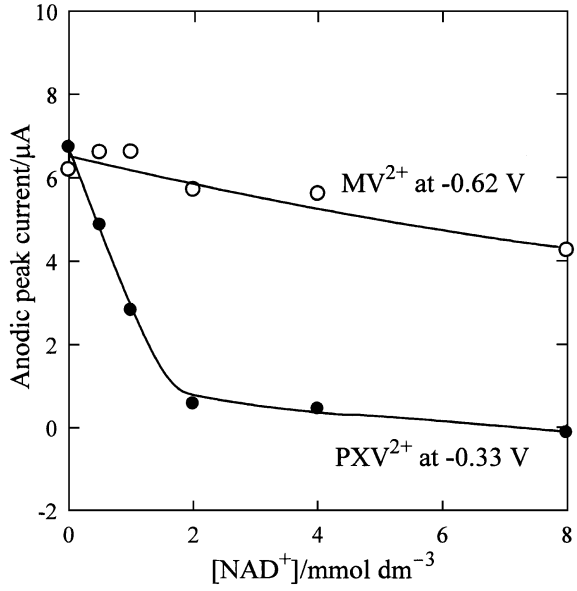

Fig. 4. Changes in the anodic current at the anodic wave peak, observed during the forward positive scan in the absence of NAD^+, vs. the concentrations of NAD^+ added. Cyclic voltammetric conditions were the same as in Fig. 3.

for the mixture with PXV^{2+} and at −0.62 V for the mixture with MV^{2+} during the forward positive scan were both lowered in the presence of the added NAD^+. The decrease in the anodic current was particularly observed in the NAD^+–PXV^{2+} mixture. The NAD^+ concentration dependence of the anodic current decrease is exhibited in Fig. 4.

Fig. 5 shows the in situ absorption spectra, recorded in the period of applying −1.1 V (vs. Ag-quasi-reference electrode) to the OTTLE cell filled with the 4.0 mmol dm^{-3} NAD^+ solution in the presence and absence of viologen and in the following period of 280 s with no potential application. Fig. 5 (inset) shows the time courses for the change in absorbance of interest. The change in the absorbance at 340 nm (A_{340}) was particularly given attention in connection with the formation of NADH. In the reaction with no viologens (Fig. 5A), the absorption band around 340 nm occurred by applying −1.1 V (vs. Ag-quasi-reference electrode) and it began to simply drop soon after stopping it.

In the case of the NAD^+–MV^{2+} mixture (Fig. 5B), the spectral change pattern resembled that for the system with no NAD^+. It is noted, however, that the peaks at 394 and

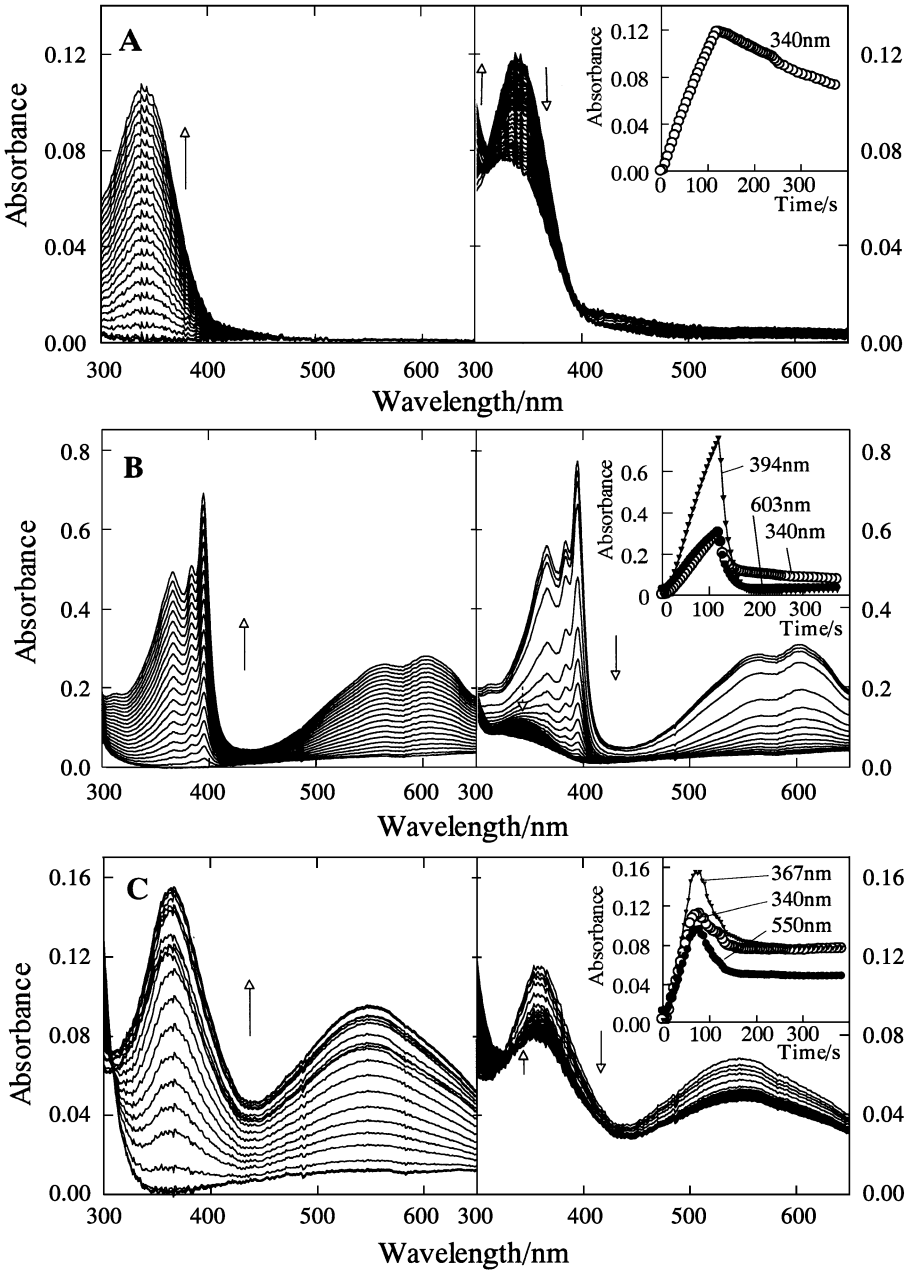

Fig. 5. In situ absorption spectra for 0.1 mol dm^{-3} KCl solutions containing NAD^+ (10.0 mmol dm^{-3}) alone (A), NAD^+ (10.0 mmol dm^{-3})–MV^{2+} (2.0 mmol dm^{-3}) mixture (B), and NAD^+ (10.0 mmol dm^{-3})–PXV^{2+} (50 μmol dm^{-3}) mixture (C). Potential applied, −1.1 V vs. Ag-quasi-reference electrode. The potential was applied for the initial 2 min and then stopped. Inset, time courses for the absorbance at the given wavelengths.

Table 1
Relative light emission intensity relating to the amounts of the enzymatically active NADH formed at the time elapsed after the electrolysis at the given potential[a]

Time (min)[b]	− 0.70 V	− 0.90 V	− 1.10 V
0	0.57	0.53	0.43
10	0.81	0.95	0.86
20	0.81	1.00[c]	0.95
50	0.57	0.94	0.76

[a] Electrolysis at given potentials was carried out in the air-equilibrated 0.1 mol dm^{-3} KCl solution containing 4.0 mmol dm^{-3} NAD^+ and 50 μmol dm^{-3} PXV^{2+} for 10 min (see also Section 2.4).
[b] Time elapsed after the electrolysis at the given potential.
[c] Relative light emission intensity was normalized to the intensity at − 0.9 V and at 20 min (= 1.00).

603 nm decreased steeply by stopping the potential application. By contrast, the decrease in A_{340} was slow.

As seen in Fig. 5C, both bands peaking at 367 and 550 nm, caused by the electroreduction of PXV^{2+}, rapidly decreased soon after they reached maximum. Importantly, the A_{340} alone exhibited an upward curvature in the latter half of the time course, although the increase in A_{340} was slight.

3.4. Evaluation for enzymatically active NADH

Relative intensity of the light emission arising from the NADH/FMN oxidoreductase coupled luciferase reaction with the NAD^+–PXV^{2+} mixture, electrolyzed at the fixed potentials and then treated with $PAASO_3^-$, are summarized in Table 1. It is worthy to note that the light emission from the luciferase reaction with the mixture, which was withdrawn at about 10–20 min after the electrolysis and treated with $PAASO_3^-$, was about two times stronger than that with the mixture, withdrawn just after the electrolysis and similarly treated. No light emission was observed in the similar reaction using a mixture with no electrolysis. Regarding the NAD^+–MV^{2+} mixture after being electrolyzed, it gave rise to only a faint light emission in the luciferase reaction, carried out in a similar manner.

4. Discussion

As well studied, MV^{2+} is subject to the two-step electroreduction to yield the neutral MV via the formation of $MV^{+\cdot}$ [18,19,29], being indicated in Fig. 1. Taking into this consideration, the two defined redox waves for PXV^{2+} indicate that PXV^{2+} likewise undergoes the two-step electroreduction via the formation of $PXV^{+\cdot}$. Furthermore, on the basis of the finding that the two cathodic waves for PXV^{2+} are present at potentials more positive than those for MV^{2+}, PXV^{2+} is conceivable to be much more susceptible to the electroreduction than MV^{2+}. The redox site of PXV^{2+} seems to be present in the vicinity of the surface of the PXV^{2+} molecule, which is supposed to be a linear macromolecule consisting of 4,4′-bipyridyl and α,α′-dibromo-*p*-xylene and to take a folded structure in aqueous solution because of the hydrophobic interaction among xylene units.

The fact that the peak cathodic current for $1e^-$ reduction of PXV^{2+} is about 5 times greater than that of MV^{2+} even when the concentration of the viologen moiety of PXV^{2+} is about one order lower than that of MV^{2+} (Fig. 1) may suggest that the cathodic wave is mainly due to the reduction of PXV^{2+} adsorbed on the electrode. Relating to this, the observation that the maximal potential for the first cathodic wave of PXV^{2+} slightly shifts, depending on the potential scan rate (Fig. 1, inset), may suggest that the first step reduction of PXV^{2+} is somewhat affected by its conformational change in the adsorption interaction between PXV^{2+} and the electrode. By contrast, the scan-rate dependency of the second cathodic wave of PXV^{2+} is absent, possibly suggesting that further $1e^-$ reduction of $PXV^{+\cdot}$ is free from the plausible conformational change at the electrode. The fact that the electroreduction of MV^{2+} exhibits the scan rate dependency opposite to that of PXV^{2+} might be due to that the second step is prone to be deviate from the redox behaviors as compared to the first step $1e^-$ reduction.

As judged by the first cathodic wave (Fig. 1), the applied potential of − 1.1 V (vs. Ag-quasi-reference electrode; corresponding to ca. − 0.76 V vs. Ag/AgCl) chosen for the spectropotentiometric measurement is expected primarily to cause the first step reduction in both systems. As indicated in Fig. 2, the absorption bands arose during the electroreduction of MV^{2+} is attributed to the generation of $MV^{+\cdot}$ [30]. Similarly, it is probable that $PXV^{+\cdot}$ is responsible for the absorption band with maxima at 367 and 550 nm. Contrary to the case of $MV^{+\cdot}$, the absence of the fine structures might be due to the vibration relaxation in the polymer matrix.

A noticeable feature that the k_{app} value for the absorbance drop of $PXV^{+\cdot}$ is about 200 times smaller than that of $MV^{+\cdot}$ may indicate that $PXV^{+\cdot}$ stably persists in the microenvironment of the polymer. This may be explained by the idea that the reoxidation of $PXV^{+\cdot}$ with the dissolved O_2 is much slower than that of $MV^{+\cdot}$, being supported by the fact that the redox potential of $PXV^{2+}/PXV^{+\cdot}$ (ca. − 0.20 V vs. Ag/AgCl (3.3 mol dm^{-3} KCl)) is more positive than that of $MV^{2+}/MV^{+\cdot}$ (ca. − 0.64 V). Moreover, it is postulated that the polymer microenvironment is favorable to retard the radical annihilation between the viologen radical sites. Likewise, the fact that the rise in the absorption bands characteristic of $PXV^{+\cdot}$ are rather faster than those of $MV^{+\cdot}$ might be due to the difference in the reoxidation and/or annihilation properties between $PXV^{+\cdot}$ and $MV^{+\cdot}$, i.e., $PXV^{+\cdot}$ is supposed to be much more tolerant toward reoxidation and radical annihilation than $MV^{+\cdot}$. The anticipated high stability of $PXV^{+\cdot}$ would be favorable for utilizing the $PXV^{2+/+\cdot}$ couple as a redox electron-transfer mediator.

The observation that the peak anodic current at − 0.33 V in the cyclic voltammogram of the mixture of NAD^+ with PXV^{2+} is markedly lowered with increasing the concentra-

tion of the added NAD^+ (Figs. 3 and 4) suggests that the electrogenerated $PXV^{+\cdot}$ transfers its electron to NAD^+ and/or to its $1e^-$ reduced form, $NAD^\cdot$, possibly leading to the formation of NADH as expressed by Eqs. (3) and (4), both of which seem to also be applicable to the system with MV^{2+}.

$$NAD^+ + 2PXV^{+\cdot} + H^+ \rightarrow NADH + 2PXV^{2+} \quad (3)$$

$$NAD^\cdot + PXV^{+\cdot} + H^+ \rightarrow NADH + PXV^{2+} \quad (4)$$

From the cyclic voltammetric observation that a cathodic wave maximum for NAD^+ in 0.1 mol dm^{-3} KCl is present at about -0.71 V (data not shown), probably due to the generation of $NAD^\cdot$ [31], both NAD^+ and $NAD^\cdot$ seem possible to be fed with electron by $PXV^{+\cdot}$. Such ET reactions will regenerate PXV^{2+} at the solution–electrode interface, resulting in depletion of $PXV^{+\cdot}$. Assuming that the $PXV^{+\cdot}$ mediated reaction proceeds favorably, much larger cathodic peak due to the reduction of the regenerated PXV^{2+} should be observed during the scan back, but no large cathodic wave is present (Fig. 3). Although the reason why the cathodic wave is absence is not clear at present, there could be a possibility that the adsorption interaction between PXV^{2+} and the electrode surface is prone to be suppressed in the presence of excess NAD^+.

By applying sufficiently negative potentials to the electrode, $PXV^{+\cdot}$ is resultingly produced to react possibly with both NAD^+ and $NAD^\cdot$. As a result of the mediated reaction, $PXV^{+\cdot}$ is converted to PXV^{2+}, being supported by the fact that the anodic wave for $PXV^{+\cdot}$ becomes much smaller. It is also noted that there is no significant difference in the cathodic current at the end of the cyclic potential scan (-0.9 V) due to the reduction of NAD^+, being overlapped with the current due to the reduction of PXV^{2+}, between two systems with 2 mmol dm^{-3} NAD^+ and with 8 m mol dm^{-3} NAD^+ (Fig. 3). This might also suggest that that NAD^+ and/or $NAD^\cdot$ are consumed in the mediated reaction with $PXV^{+\cdot}$. By contrast, the findings that (i) the MV^{2+}–NAD^+ system exhibits the relatively large anodic wave during the positive potential scan carried out after the pretreatment and that (ii) the cathodic current at the end of the potential scan considerably increases with an increase in the NAD^+ concentration would suggest that the $MV^{+\cdot}$ mediated reaction is less efficient than that of the mediated reaction with $PXV^{+\cdot}$.

The in situ absorption spectra for the NAD^+ solution with and with no viologens provided significant information on the reaction between viologens and NAD^+. With no viologens, the absorption band peaking around 340 nm, arisen by applying -1.1 V (vs. Ag-quasi-reference electrode), may be associated mainly with the dimer, $(NAD)_2$, formed via coupling of $NAD^\cdot$ [31,32]. Besides the dimer, the $2e^-$ reduced product, NADH, is supposed to be partly responsible for the increase in A_{340}. The decrease in A_{340}, begun soon after cessation of the potential application, might be due to the oxidative breakdown of $(NAD)_2$ with O_2 [32].

For the system with MV^{2+} or PXV^{2+}, the reaction of $V^{+\cdot}$ not only with NAD^+ but also with $NAD^\cdot$, leading to formation of NADH (Eqs. (3) and (4)), is conceivable to cause the steep decrease observed immediately after cessation of the potential application.

As seen in Fig. 5B and C (insets), the decrease in A_{340} is slower than that in the A values at the maximal wavelengths. This is observed particularly in the system with PXV^{2+}, which also exhibited the faint increase in A_{340} in the latter half of the time course, where no electrogeneration of $NAD^\cdot$ proceeds. This may indicate that the chemical reaction between NAD^+ and $PXV^{+\cdot}$ with relatively long lifetime as mentioned above is primarily responsible for the formation of NADH. This anticipation is sustained by the bioluminescence assay results (i) that the light emission with the reaction mixture, withdrawn at 10–20 min after cessation of the electrolysis and treated with $PAASO_3^-$, is enhanced about twofold as compared to that with the similarly treated reaction mixture sampled immediately after the electrolysis, and (ii) that the reaction mixtures via the electrolysis at -0.9 V, of which potential is supposed to be the most efficient for the electrogeneration of $PXV^{+\cdot}$ of the three tested potentials (Fig. 1), give rise to the most intense light except the conditions at -0.7 V and at 0 min (Table 1). The exceptional case might be explained by assuming that the concentration of NAD^+, being available in the reaction expressed by Eq. (3), just after stopping the electrolysis at -0.7 V is greater than that at -0.9 V.

5. Conclusions

Based on the results mentioned above, we conclude (i) that PXV^{2+} is an attractive ET mediator candidate, being able to function in the solution phase, and (ii) that the ET reaction between $PXV^{+\cdot}$ and NAD^+ permits the generation of the enzymatically active NADH. From these results, it also seems that the water-soluble viologen polymer has a possibility to become a useful ET mediator. We are currently studying the detailed mechanism for the ET reaction, while taking into consideration of its efficiency, with the aid of the MNDO-PM3 molecular orbital method.

References

[1] K. Kamata, T. Suzuki, T. Kawai, T. Iyoda, Voltammetric anion recognition by a highly cross-linked polyviologen film, J. Electroanal. Chem. 473 (1999) 145–155.
[2] D. Kirstein, L. Kirstein, F. Scheller, H. Borcherding, J. Ronnenberg, S. Diekmann, P. Steinrucke, Amperometric nitrate biosensors on the basis of *Pseudomonas stutzeri* nitrate reductase, J. Electroanal. Chem. 474 (1999) 43–51.
[3] S.C. Glazier, E.R. Campbell, W.H. Campbell, Construction and characterization of nitrate reductase-based amperometric electrode and nitrate assay of fertilizer and drinking water, Anal. Chem. 70 (1998) 1511–1515.
[4] H. Imahori, H. Yamada, Y. Nishimura, I. Yamazaki, Y. Satake, Vec-

trial multistep electron transfer at the gold electrodes modified with self-assembled monolayers of ferrocene–porphyrin–fullerene triads, J. Phys. Chem., B 104 (2000) 2099–2108.
[5] M. Suzuki, M. Kimura, K. Hanabusa, H. Shirai, Enhancement effects of L-tyrosine esters on photosensitized separation using ruthenium(II) complex- and viologen-containing polymers, Polymer 42 (2001) 9235–9241.
[6] M. Kaneko, Charge transport in solid polymer matrixes with redox centers, Prog. Polym. Sci. 26 (2001) 1101–1137.
[7] I. Willner, B. Willner, Artificial photosynthetic model systems using light-induced electron transfer reactions in catalytic and biological assemblies, Top. Curr. Chem. 159 (1991) 154–218.
[8] H. Tatsumi, K. Takagi, M. Fujita, K. Kano, T. Ikeda, Electrochemical study of reversible hydrogenase reaction of *Desulfovibrio vulgaris* cells with methyl viologen as an electron carrier, Anal. Chem. 71 (1999) 1753–1759.
[9] P.-C. Maness, P.F. Weaver, Evidence for three distinct hydrogenase activities in *Rhodospirillum rubrum*, Appl. Microbiol. Biotechnol. 57 (2001) 751–756.
[10] D. Mandler, I. Willner, Solar light induced formation of chiral 2-butanol in an enzyme-catalyzed chemical system, J. Am. Chem. Soc. 106 (1984) 5352–5353.
[11] D. Mandler, I. Willner, Photosensitized NAD(P)H regeneration systems; application in the reduction of butan-2-one, pyruvic, and acetoacetic acids and in the reductive amination of pyruvic and oxoglutaric acid to amino acid, J. Chem. Soc., Perkin Trans., II (1986) 805–811.
[12] M. Abo, M. Dejima, F. Asano, A. Okubo, S. Yamazaki, Electrochemical enzymatic deoxygenation of chiral sulfoxides utilizing DMSO reductase, Tetrahedron: Asymmetry 11 (2000) 823–828.
[13] K. Delecouls-Servat, R. Basseguy, A. Bergel, Designing membrane electrochemical reactors for oxidoreductase-catalysed synthesis, Bioelectrochemistry 55 (2002) 93–95.
[14] R.J. Fisher, J.M. Fenton, J. Iranmahbood, Electro-enzymatic synthesis of lactate using electron transfer chain biomimetic membranes, J. Membr. Sci. 177 (2000) 17–24.
[15] S. Kim, S.-E. Yun, C. Kang, Electrochemical evaluation of the reaction rate between methyl viologen mediator and siaphorase enzyme for the electrocatalytic reduction of NAD^+ and digital simulation for its voltammetric responses, J. Electroanal. Chem. 462 (1999) 153–159.
[16] S. Suye, Y. Aramoto, M. Nakamura, I. Tabata, M. Sakakibara, Electrochemical reduction of immobilized $NADP^+$ on a polymer modified electrode with a co-polymerized mediator, Enzyme Microb. Technol. 30 (2002) 139–144.
[17] Z. Samec, W.T. Bresnahan, P.J. Elving, Theortical analysis of electrochemical reactions involving two successive one-electron transfers with dimerization of intermediate-application to NAD^+/NADH redox couple, J. Electroanal. Chem. 133 (1982) 1–23.
[18] O. Enea, Adsorption of the *N*,*N*′-dimethyl-4,4′-bipyridinium cation (MV^{2+}) and of the $[Rh(bpy)_3]^{3+}$ complex on Pt, Au and Pt+Au electrodes, Electrochim. Acta 30 (1985) 13–16.
[19] G.S. Ostrom, D.A. Buttry, Quartz crystal microbalance studies of deposition and dissolution mechanism of electrochromic films of diheptylviologen bromide, J. Electroanal. Chem. 256 (1988) 411–431.
[20] K. Shimazu, M. Yanagida, K. Uosaki, Simultaneous UV–Vis spectroelectrochemical and quartz crystal microgravimetric measurements during the redox reaction of viologens, J. Electroanal. Chem. 350 (1993) 321–327.
[21] V. Reipa, S.-M.L. Yeh, H.G. Monbouquette, V.L. Vilker, Reorientation of tetradecylmethyl viologen on gold upon coadsorption of decanethiol and its mediation of electron transfer to nitrate reductase, Langmuir 15 (1999) 8126–8132.
[22] A.L. De Lacey, M. Detcheverry, J. Moiroux, C. Bourdillon, Construction of multicomponent catalytic films based on avidin–biotin technology for the electroenzymatic oxidation of molecular hydrogen, Biotechnol. Bioeng. 68 (2000) 1–10.
[23] H. Keith Chenault, G.M. Whitesides, Regeneration of nicotinamide cofactors for use in organic synthesis, Appl. Biochem. Biotechnol. 14 (1987) 147–197.
[24] A. Factor, G.E. Heinsohn, Polyviologens—a novel class of cationic polyelectrolyte redox polymers, Polym. Lett. 9 (1971) 289–295.
[25] H. Karatani, T. Konaka, C. Katsukawa, Properties of the bimodal fluorescent protein produced by *Photobacterium phosphoreum*, Photochem. Photobiol. 71 (2000) 230–236.
[26] H. Karatani, Y. Tsujimura, S. Hirayama, Electron-link between bacterial luciferase and electrochemically sensitized $Ru(bpy)_3^{2+}$*-methylviologen system within Nafion membrane, Chem. Lett. (2002) 468–469.
[27] J.W. Hastings, T.O. Baldwin, M.Z. Nicoli, Bacterial luciferase: assay, purification, and properties, Methods Enzymol. 57 (1978) 135–152.
[28] E. Jablonski, M. DeLuca, Purification and properties of the NADH and NADPH specific FMN oxidoreductases from *Benekea harveyi*, Biochemistry 16 (1977) 2932–2936.
[29] N.F. Ferreyra, S.A. Dassie, V.M. Solis, Electroreduction of methyl viologen in the presence of nitrite. Its influence on enzymatic electrodes, J. Electroanal. Chem. 482 (2000) 126–132.
[30] J.W. Strojek, G.A. Gruver, T. Kuwana, Direct log ratio recording scanning spectrophotometer, Anal. Chem. 41 (1969) 481–484.
[31] M.A. Jensen, P.J. Elving, Nicotinamide adenine dinucleotide (NAD^+): formal potential of the $NAD^+/NAD^{\cdot}$ couple and $NAD^{\cdot}$ dimerization, Biochim. Biophys. Acta 764 (1984) 310–315.
[32] R.W. Burnett, A.L. Underwood, A dimer of diphosphopyridine nucleotide, Biochemistry 7 (1968) 3328–3333.